J. Fluid Mech. (1989), *vol.* 202, *pp.* 233–261
Printed in Great Britain

Measurements of heat diffusion from a continuous line source in a uniformly sheared turbulent flow

By U. KARNIK AND S. TAVOULARIS
Department of Mechanical Engineering, University of Ottawa, Ottawa, Canada

(Received 16 February 1988 and in revised form 30 August 1988)

The diffusion of a passive scalar (heat) from a continuous line source placed in a uniformly sheared, nearly homogeneous, turbulent shear flow is examined. Measurements indicate that the mean temperature profile is approximately Gaussian near the source but, further downstream, it becomes asymmetric and its peak shifts towards the region of lower velocity. The r.m.s. temperature fluctuation profile is double peaked close to the source, it is single peaked at intermediate distances and it demonstrates a re-emergence of double peaks which grow in relative magnitude far away from the source. In comparison to similar experiments in isotropic turbulence, the centreline mean temperature appears to have a comparable decay rate, whereas the centreline mean-square temperature fluctuations appear to decay at a faster rate. The spread of the plume is faster than that in isotropic turbulence. The measured turbulent heat fluxes and triple temperature–velocity correlations demonstrate self-similar features. The development of temperature integral lengthscales and microscales is comparable to that in other heated, uniformly sheared flows, while the temperature p.d.f. and the temperature–velocity joint p.d.f. are distinctly non-Gaussian, especially away from the centreline. The relative magnitudes of the two measured components of the turbulent diffusivity tensor are in agreement with earlier measurements.

1. Introduction

The efficiency of turbulence in mixing and transporting scalars such as heat, moisture, chemical reactants and pollutants has provided the motivation for much turbulence research. Since the pioneering work of Taylor (1921), numerous theoretical, experimental and numerical studies have dealt with the problem of turbulent diffusion. The diffusion of heat released from thin sources in nearly isotropic, grid turbulence has been studied by Schubauer (1935), Collis (1948), Frenkiel (1950), Townsend (1951, 1954), Uberoi & Corrsin (1952), Shlien & Corrsin (1974), Warhaft (1984) and Stapountzis *et al.* (1986), whereas Kistler (1956) and Warhaft (1981, 1984) have studied the dispersion of heat from two fixed line sources in grid turbulence. Experiments in grid turbulence with a uniform mean temperature profile have been performed by Kistler, O'Brien & Corrsin (1956), Mills *et al.* (1958), Mills & Corrsin (1959), Yeh & Van Atta (1973), Lin & Lin (1973), Sepri (1976), Newman, Warhaft & Lumley (1977), Warhaft & Lumley (1978) and Sreenivasan *et al.* (1980), whereas cases with a uniform mean temperature gradient have been reported by Wiskind (1962), Alexopoulos & Keffer (1971), Venkataramani & Chervay (1978), Sirivat & Warhaft (1983), and Budwig, Tavoularis & Corrsin (1985). Numerical simulations complementing these experimental investigations include, among others, the work by Libby & Scragg (1972), Sullivan (1976), Lumley (1978,

1983), Anand & Pope (1983), Pope (1981, 1983), Lumley & Van Cruyningen (1985) and Shih & Lumley (1986).

Corrsin (1952) was probably the first to examine the diffusion of scalars in sheared homogeneous turbulence. Theories on turbulent diffusion in shear flows have been reviewed by Hinze (1975) and Monin & Yaglom (1973). A number of the available analyses and experiments have considered the case with a constant mean temperature gradient superimposed on the velocity field. Analyses of such flows have been presented, among others, by Deissler (1962), Fox (1964) and Tavoularis & Corrsin (1985). The experiments of Tavoularis & Corrsin (1981 *a*, *b*) provide a detailed documentation of such a flow; Sreenivasan, Tavoularis & Corrsin (1981) have focused their attention on evaluating the performance of gradient transport models whereas Tavoularis & Corrsin (1985) have concentrated on the effect of mean shear on the diffusivity tensor. Riley & Corrsin (1974) have attempted to relate the turbulent diffusivities to the Lagrangian velocity statistics whereas Riley & Corrsin (1971), Jones & Musonge (1983), Shirani, Ferziger & Reynolds (1981) and Rogers, Moin & Reynolds (1986) have presented numerical analyses for scalar transport in uniformly sheared flows.

Analytical studies of the diffusion from concentrated sources in a uniformly sheared flow have been presented by Novikov (1958), Elrick (1962), Okubo & Karweit (1969) and Huang (1979). While the present investigation was in progress, a few relevant experimental studies also appeared. These include the point-source measurements by Nakamura *et al.* (1986) and Sakai *et al.* (1986) and the line-source measurements by Stapountzis & Britter (1987) and Kyong & Chung (1987 *a*, *b*). Concerning the latter two experiments, one may note that Stapountzis & Britter (1987) provide measurements only relatively close to the source while the results of Kyong & Chung (1987 *a*, *b*) appear to be affected by the wake of the heated source. The only other available experiments are the preliminary results of Tavoularis & Corrsin (1981 *a*), using a single heating rod in their shear generator.

In the present experiments, the diffusion of heat from a line source in the presence of a uniform mean shear is studied. Although it is well known that exact transverse homogeneity is incompatible with the preservation of uniform shear (Champagne, Harris & Corrsin 1970; Harris, Graham & Corrsin 1977), the present flow field exhibits improved homogeneity compared to those in previous studies. The velocity field as well as the mean and fluctuating temperature fields are documented in detail. Having already established the fact that the velocity field attains a self-similar structure asymptotically (Tavoularis & Karnik 1989), it seemed worthwhile to investigate whether the temperature field is also self-similar. Furthermore, the present study provides temperature–velocity joint statistics such as heat fluxes and higher correlations as well as probability density functions with the purpose of documenting in depth the diffusion process and also generating a reliable database for future tests of theoretical and computational models.

2. Experimental facility

A detailed description of the wind tunnel used in the present investigations has been provided by Karnik & Tavoularis (1987). The flow, produced by two centrifugal blowers, passed through various turbulence reduction screens and a 16:1 contraction before entering the test section shown in figure 1. The velocity profile was produced with the use of a shear generator which consisted of 12 channels with adjustable resistance within each channel. To obtain uniformity of scales, the flow was directed

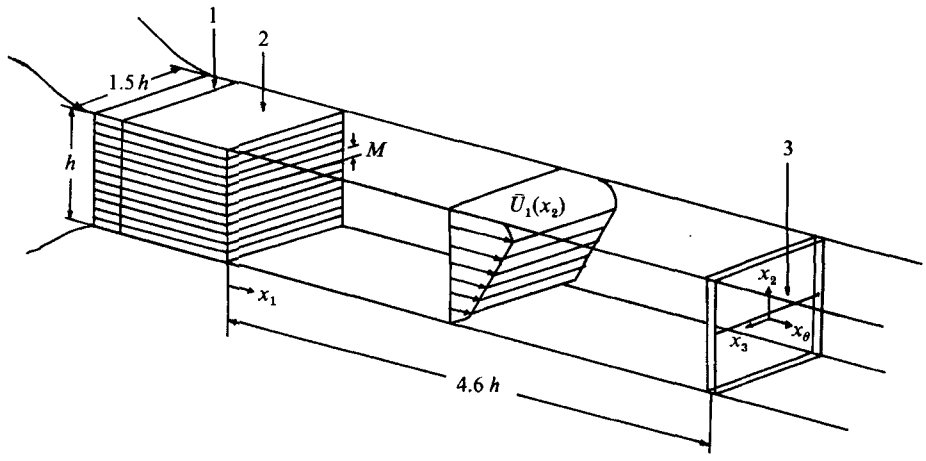

FIGURE 1. Sketch of the wind-tunnel test section. (1) Shear generator, (2) flow separator, (3) heating source. $M = 0.0254$ m, $h = 0.305$ m.

through a flow separator, consisting of 12 unobstructed channels which were aligned with those in the shear generator. The height, M, of each individual channel (including half-thickness of separating plates) was 25.4 mm. This quantity is indicative of the typical turbulent eddy size and analogous to the mesh size in grid turbulence. The test section was equipped with four slots for the insertion of frames fitted with the flow manipulators or heaters. The vertical walls of the downstream part of the test section were adjusted to partially compensate for boundary-layer growth.

Heat was introduced by electrically heating a metallic element, stretched across the vertical walls of a wooden frame which could be inserted into the slots provided in the wind-tunnel test section. The element was held fixed at one end and was kept taut with the use of small weights suspended at the free end. In all the present experiments, the distance of the element from the flow separator was $4.6h$, where $h = 0.305$ m is the height of the test section.

For measurements close to the source, a nichrome wire with diameter $d = 0.051$ mm and supplied with electric power of approximately 7 W/m was used. At a mean centreline velocity $\bar{U}_{1c} = 13.0$ m/s, the Reynolds number, based on the kinematic viscosity of the air in the vicinity of the heated wire, was estimated to be 22, lower than the critical value of 40 above which vortex shedding might occur. It was found, however, that in order to generate measurable temperature signals at large downstream distances, it would be necessary to release more heat than a single cylindrical wire could withstand in the low-Reynolds-number regime. Thus, a heating ribbon (toaster element) was used as a source; it had a thickness of 0.13 mm and a width of 0.528 mm, and was provided with approximately 70 W/m power. It was expected that the temperature field of this source would approximate that of a line source at a sufficient downstream distance. The Reynolds number based on the thickness of the element and at the mean speed of 7.8 m/s used for these tests was approximately 67 at ambient temperature and approximately 15 at the film temperature, low enough for the possibility of vortex shedding with the ribbon considered as a bluff body to be ruled out.

The mean temperature was measured by glass-coated thermistor mini-probes (Fenwall Electronics, 2000Ω), operating with home-made electronic circuits.

Variations in room temperature were accounted for by measuring the temperature rise above the ambient flow temperature, which was monitored upstream of the heating source. The fluctuating temperature was measured with a 1.3 μm platinum wire (Dantec type 55P31) operating at a constant current of 0.32 mA supplied by an active bridge (Tavoularis 1978). The cold-wire signal was amplified with a gain of 5000 and low-pass filtered at 3 kHz. The r.m.s. output of the cold wire in the unheated flow, consisting almost entirely of electronic noise, was equivalent to a r.m.s. temperature fluctuation, θ'_n, of approximately 0.013 °C. The mean-squared temperature fluctuations were corrected by subtracting θ'^2_n from the corresponding raw measurement based on the assumption that the temperature fluctuations and noise were uncorrelated.

The velocity field was measured with a custom-made miniature cross-wire array (TSI model 1248BJT1.5). The 5 μm diameter wires were approximately 2 mm long and 0.51 mm apart and were powered by two TSI 1050 constant-temperature anemometers. The instantaneous effective cooling velocity, U_{eff}, of each wire was obtained from the anemometer output voltage, E, by inverting the modified King's law as

$$U_{\text{eff}} = \left[\left(\frac{E^2}{\overline{T}_{\text{w}} - \overline{T}_{\text{f}} - \theta_{\text{f}}} - A\right)\Big/ B\right]^{1/n}, \tag{1}$$

where $\overline{T}_{\text{w}}$ is the hot-wire temperature, equal to about 250°, $\overline{T}_{\text{f}}$ and θ_{f} are the mean and instantaneous temperature fluctuations of the flow and A, B and n are calibration constants. The addition and subtraction of the values of U_{eff} for each wire provided instantaneous values of the streamwise and transverse velocity components.

Measurements of U_{eff} were corrected for the temperature sensitivity by incorporating the values of $\overline{T}_{\text{f}}$ and θ_{f} measured with the thermistor mini-probe and the cold wire placed alongside the cross-wire array. The cold wire was positioned on the (x_θ, x_3)-plane with its axis at an angle of approximately 5° with respect to the x_3 axis; its centre was aligned with the centres of the cross-wire array and was about 2 mm away from the closest hot-wire sensor. The bead of the mini-thermistor probe was also aligned with the wire centres along the x_3 axis. A data acquisition system, consisting of a PC-controlled, high-speed, analog-to-digital I/O board (DT2828, Data Translation Inc.) was used to digitize and process the signals.

3. Measurements

3.1. *The velocity field*

Detailed measurements published earlier (Karnik & Tavoularis 1987) have established the downstream constancy and the spanwise uniformity of the mean shear. A study of the turbulent characteristics is presented by Tavoularis & Karnik (1989).

Although, as mentioned earlier, exact transverse homogeneity is not possible in unbounded uniformly sheared flows, it was desirable to have the least possible inhomogeneity within the region of interest in order to isolate the effect of mean shear on diffusion. Further improvement of the homogeneity level reported in (Tavoularis & Karnik 1989) was accomplished by finely adjusting the screens in the shear generator. Although, as expected, the mean shear was sensitive to such changes, figure 2 shows that a clearly improved transverse homogeneity was achieved with only a slight distortion of the mean shear, which remained reasonably uniform and maintained downstream a near constancy. Confirmation of the

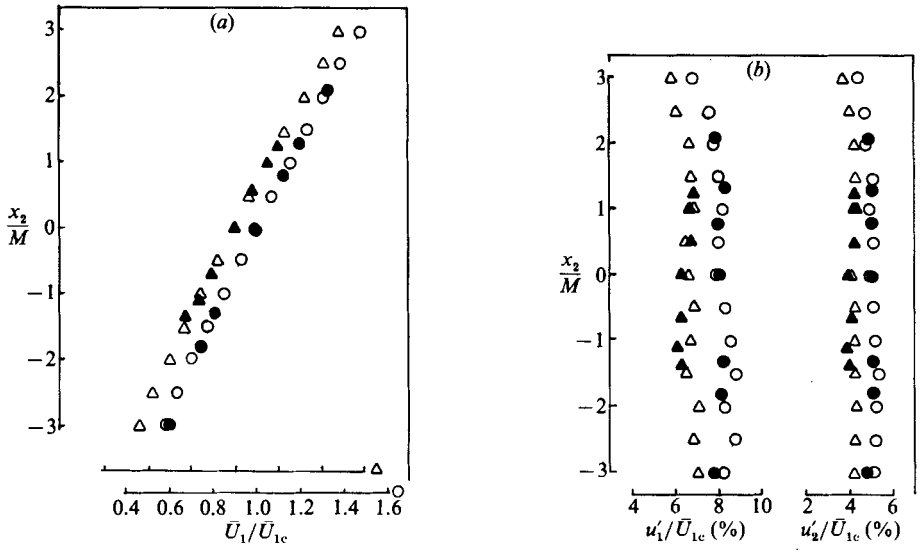

FIGURE 2. Transverse variation of (*a*) the mean velocity, (*b*) the r.m.s. velocities: △, ▲, $x_\theta/M = 48.0$; ○, ●, $x_\theta/M = 84.0$; $\bar{U}_{1c} = 7.85$ m/s; solid symbols indicate the presence of a heated source.

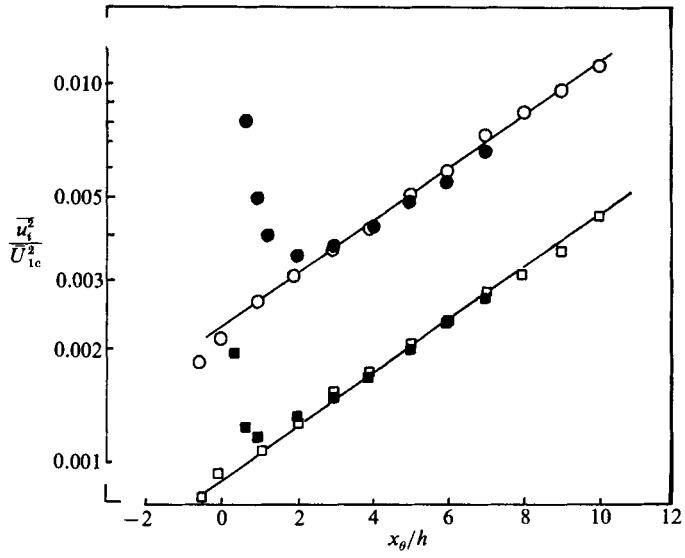

FIGURE 3. Downstream development of Reynolds stresses along the centreline; ●, ○, $\overline{u_1^2}$; ■, □, $\overline{u_2^2}$; $\bar{U}_{1c} = 7.85$ m/s; solid symbols indicate the presence of a heated source.

exponential growth (Tavoularis & Karnik 1989) of the normal Reynolds stresses is indicated in figure 3 in which x_θ is the distance downstream from the source. Figures 2 and 3 also illustrate that, except in the vicinity of the source, the velocity field was effectively unaltered by the addition of heat to the flow, thus confirming the passivity of the scalar. In all measurements reported here, the wind-tunnel constant, $k_s = (1/\bar{U}_{1c})(\mathrm{d}\bar{U}_1/\mathrm{d}x_2)$, was 0.62 ± 0.03 per m.

Figure 4 presents the transverse mean and r.m.s. velocity profile in the shear flow downstream of the ribbon. The velocity deficit was measurable near the source

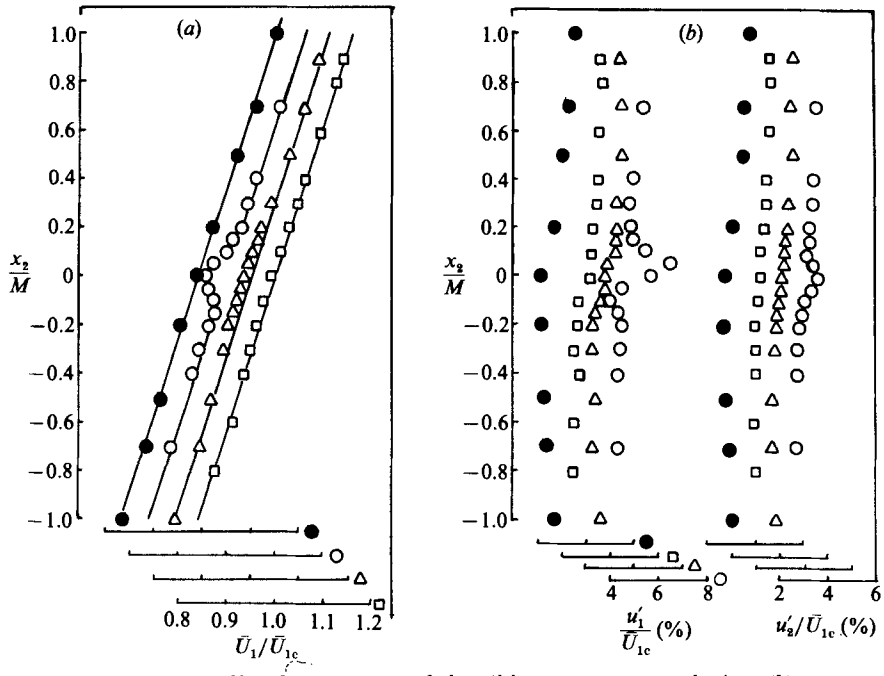

FIGURE 4. Transverse profiles downstream of the ribbon: (*a*) mean velocity, (*b*) r.m.s. velocities, $x_0/M = 0$ (●, without ribbon), 2.0 (○), 8.0 (△), 12.0 (□); $\bar{U}_{1c} = 7.85$ m/s.

($x_0/M < 12$) but not further downstream. In the case of the nichrome wire, the mean velocity deficit was measurable for $x_0/M < 3$.

3.2. *The mean temperature field*

Transverse mean temperature profiles are presented in figure 5. Following the practice used in earlier publications, the transverse positions have been normalized with the half-width, w, of the mean temperature profiles, defined as half the distance between the points having a temperature rise which is 50% of the peak value $\Delta\bar{T}_p$. For Gaussian random variables, the standard deviation of the mean profile is equal to 0.85 times the half-width. The mean temperature is normalized with the corresponding centreline temperature rise $\Delta\bar{T}_c$.

Transverse mean temperature profiles near the source at various stations downstream of the 0.051 mm diameter wire are presented in figure 5(*a*). The profiles appear to be nearly Gaussian, in conformity with the findings of Stapountzis & Britter (1987); the peaks are on the axis except very close to the wire, where a slight buoyancy effect is manifested by a shift of the peak towards positions of higher velocity. Transverse mean temperature profiles downstream of the ribbon are shown in figure 5(*b*). Near the source, except for the slight buoyancy effect, the profiles are also nearly Gaussian. However, further downstream the profiles appear to be shifted towards the region of lower velocity with the position of the peak mean temperature also shifting in the same direction. A similar observation was made by Nakamura *et al.* (1986) for diffusion from a point source in a uniform shear flow and by Kyong & Chung (1987*a*). The observation of symmetric profiles by Stapountzis & Britter (1987) is compatible with the present results, if one considers that their measurements did not extend sufficiently far from the source, where the effect of shear on diffusion would be measurable. Their observation of a shift of the peak temperature towards

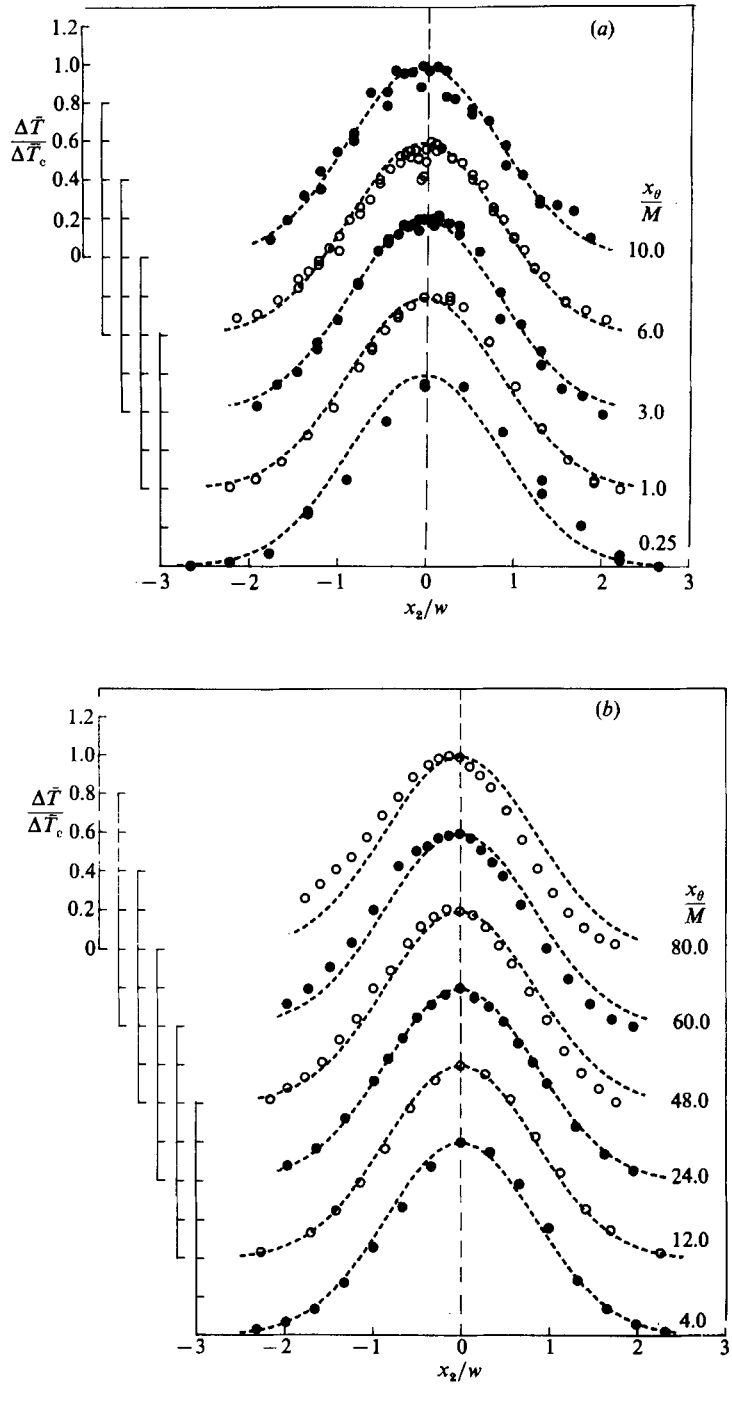

FIGURE 5. Transverse profiles of the mean temperature rise: (*a*) downstream of the 0.051 mm diameter wire, (*b*) downstream of the ribbon; ----, Gaussian profiles.

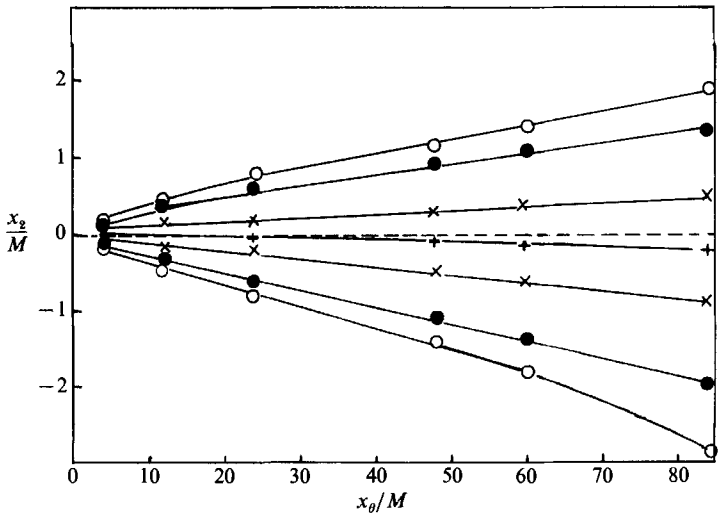

FIGURE 6. Locus of positions with $\Delta\bar{T}/\Delta\bar{T}_p = 1.0$ (+), 0.9 (×), 0.5 (●), 0.3 (○).

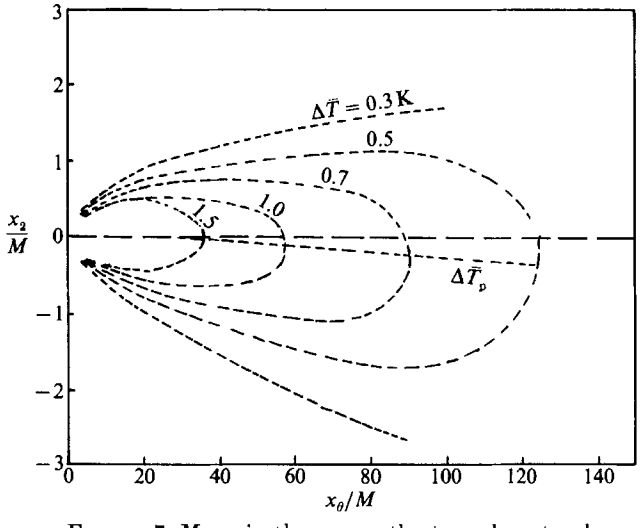

FIGURE 7. Mean isotherms on the tunnel centreplane.

the region of higher velocity could possibly be due to buoyancy rather than to shear. Further discussion on this aspect will be provided later.

Figure 6 presents the loci of points with mean temperature rise at a particular fraction of the peak mean temperature rise, $\Delta\bar{T}_p$, whereas figure 7 shows some mean isotherms on the wind-tunnel centreplane. Both these figures provide further evidence of the shift of the mean temperature profiles.

Measurements of the downstream decrease of the centreline mean temperature rise $\Delta\bar{T}_c$ are presnted in figure 8 along with measurements in isotropic turbulence (Warhaft 1984; Stapountzis *et al.* 1986) and in uniformly sheared flows (Tavoularis & Corrsin 1981*a*). These measurements have been scaled with a reference temperature rise $\Delta\bar{T}_r$, computed as

$$\Delta\bar{T}_r = \frac{P}{\rho c_p \, \mathrm{d}\bar{U}_{1c}}, \tag{2}$$

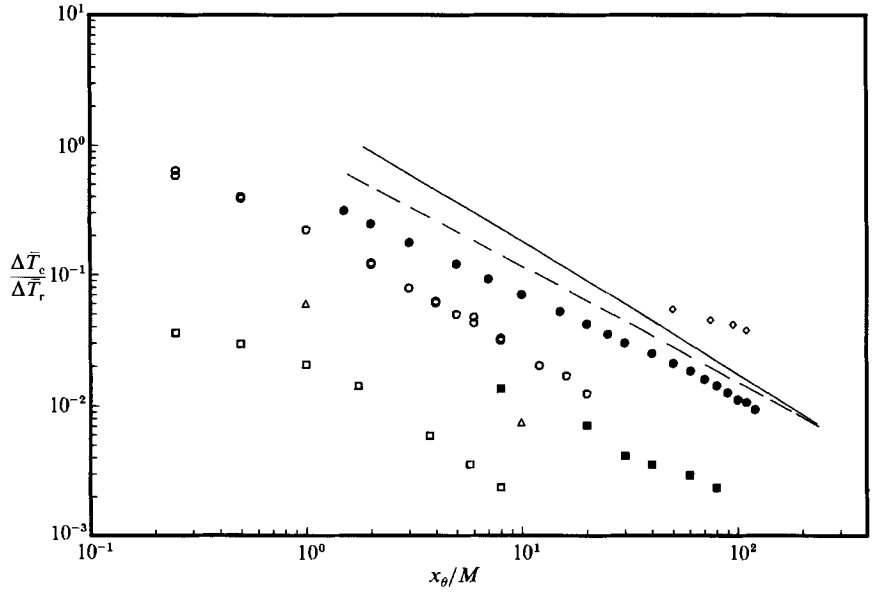

FIGURE 8. Downstream decrease of the normalized centreline mean temperature rise, $\Delta\bar{T}_c/\Delta\bar{T}_r$; ○, 0.051 mm diameter wire ($\Delta\bar{T}_r = 8.8$ °C); ●, ribbon ($\Delta\bar{T}_r = 57.3$ °C); △, Stapountzis *et al.* (1986) ($\Delta\bar{T}_r = 132.6$ °C); □, Warhaft (1984) ($d = 0.025$ mm) ($\Delta\bar{T}_r = 21$ °C); ■, Warhaft (1984) ($d = 0.127$ mm) ($\Delta\bar{T}_r = 42.3$ °C); ◇, Tavoularis & Corrsin (1981*a*) ($\Delta\bar{T}_r = 15.6$ °C); ——, $n = 1.0$; ---, $n = 0.75$.

where P is the power input to the source per unit length, d is the thickness of the source and ρ, c_p are fluid properties evaluated at ambient temperature. For simplicity, the magnitude of $\Delta\bar{T}_r$ is evaluated with the use of the measured source thickness rather than the 'effective' source thickness which depends on the geometry of the source. To facilitate comparison with the decrease of $\Delta\bar{T}_c$ in isotropic turbulence, the downstream distance was normalized with the grid or shear-generator spacing M.

It should be noted that, since the peak mean temperature rise, $\Delta\bar{T}_p$, was not appreciably different from $\Delta\bar{T}_c$, the decrease of $\Delta\bar{T}_p$ can also be deduced from figure 8. The decrease of $\Delta\bar{T}_p$ in the shear flow could be fitted, within limited ranges, by power laws of the type

$$\frac{\Delta\bar{T}_p}{\Delta\bar{T}_r} \propto \left(\frac{x_\theta}{M}\right)^{-n}. \tag{3}$$

Two distinct patterns of decay could be observed; one near the thin-wire source with $n \approx 1.0$ and the other downstream of the ribbon with $n \approx 0.75$. These exponent values are not very different from the ones observed in isotropic turbulence.

3.3. *The fluctuating temperature field*

The transverse distribution of the mean-squared temperature fluctuations is shown in figure 9. Close to the source, the profiles exhibit distinct double peaks which are suppressed in an intermediate region but reappear prominently further downstream. The peak on the side of higher velocity is greater than that on the lower side. Double peaks have also been observed in the shear flow experiments of Tavoularis & Corrsin

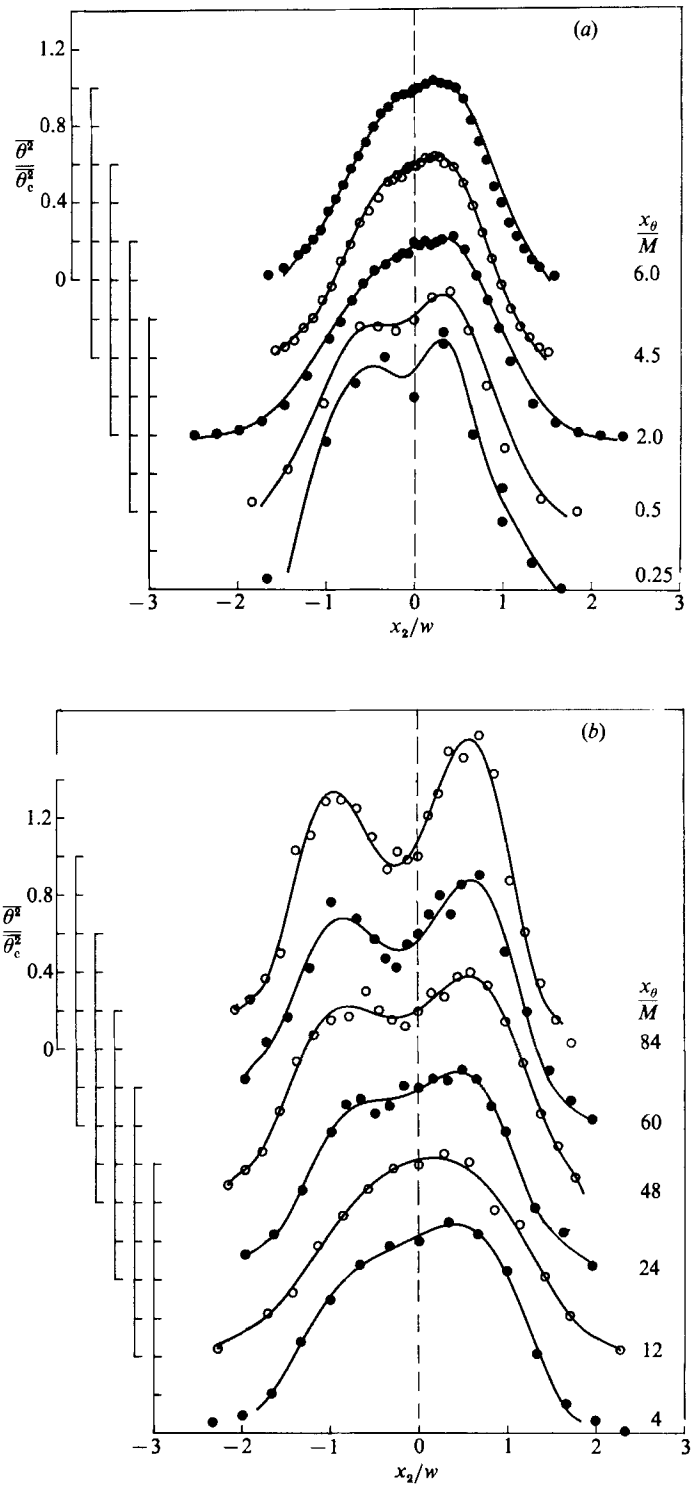

FIGURE 9. Transverse distribution of the mean-square temperature fluctuations, downstream of (*a*) the 0.051 mm diameter wire, and (*b*) the ribbon; ——, fitted curves.

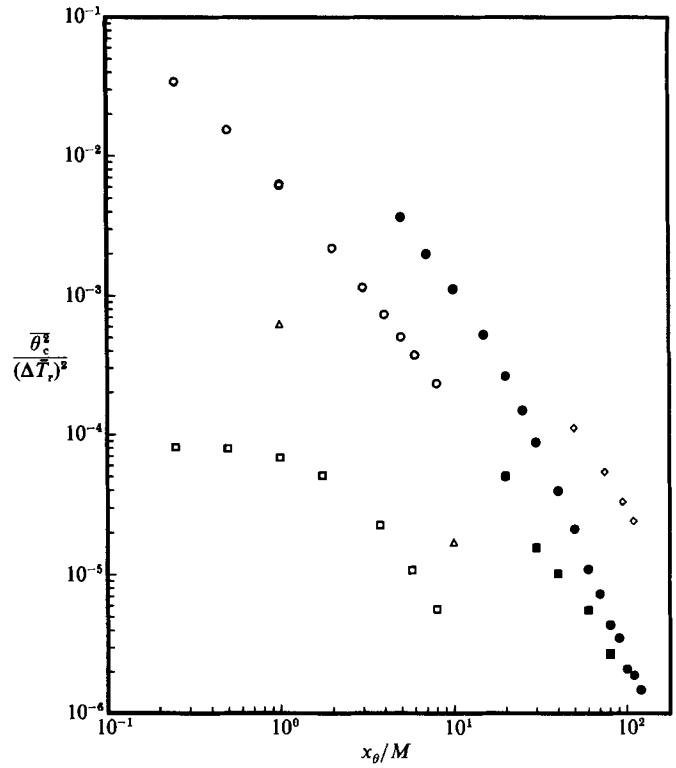

FIGURE 10. Downstream development of the normalized centreline mean-square temperature fluctuations, $\overline{\theta_c^2}/(\Delta\bar{T}_r)^2$; symbols as in figure 8.

(1981*a*) and in the isotropic turbulence experiments of Warhaft (1984). A possible explanation of double peaking will be presented in the discussion.

The downstream development of the centreline mean-squared fluctuations, $\overline{\theta_c^2}$, normalized with $(\Delta\bar{T}_r)^2$, is presented in figure 10. A simple power law of the type

$$\frac{\overline{\theta_c^2}}{(\Delta\bar{T}_r)^2} \propto \left(\frac{x_\theta}{M}\right)^{-n_\theta} \tag{4}$$

cannot be fitted to the entire range. Near the source, a value $n_\theta \approx 1.7$ seems appropriate, whereas further downstream the decay is faster, corresponding to $n_\theta \approx 3.2$. The decay close to the source is not very different from that observed in isotropic turbulence. Figure 11 indicates that the ratio of the centreline values of the r.m.s. temperature fluctuation and the mean temperature difference approaches a downstream value of 0.15, substantially lower than the value of 0.7 obtained in isotropic turbulence. The value 0.15 is also compatible with the preliminary measurements of Tavoularis & Corrsin (1981*a*).

3.4. *Integral lengthscales and microscales*

The velocity and temperature integral lengthscales were evaluated by integrating respective autocorrelation functions to their first zero and using Taylor's 'frozen flow' approximation. The scales were ensemble averaged over a number of records; each record had a duration of at least 100 times the corresponding integral timescale.

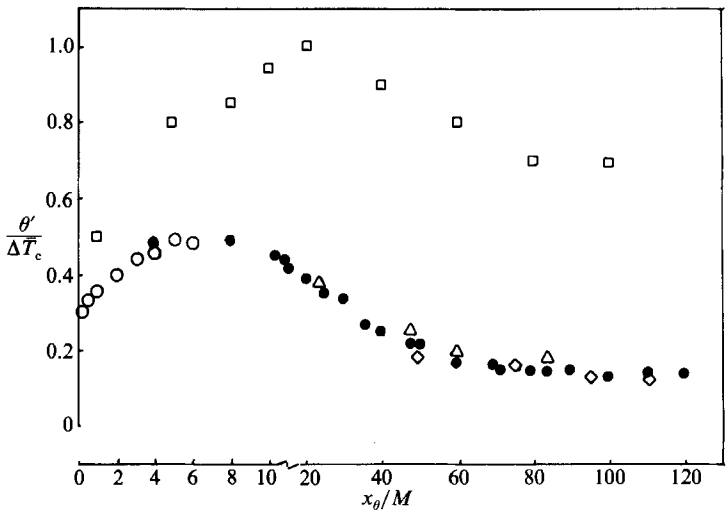

FIGURE 11. Downstream development of (i) $\theta'_c/\Delta\bar{T}_c$: ○, 0.051 mm diameter wire; ●, ribbon; □, Warhaft (1984); ◇, Tavoularis & Corrsin (1981*a*); (ii) $\theta'_p/\Delta\bar{T}_c$: △, ribbon; scale changes at $x_\theta/M = 10.0$.

The transverse distribution of the integral scales was found to be reasonably uniform.

The downstream development of the integral lengthscales along the centreline is presented in figure 12. Near the source, these scales are affected by the wake of the source but, away from it, they achieve growth rates comparable with those in the measurements of Tavoularis & Karnik (1989). The growth rate for $L_{22,1}$ is not very different from that for $L_{11,1}$ and the ratio $L_{22,1}/L_{11,1}$ is approximately 0.3, not too far from the value of 0.23 measured by Tavoularis & Corrsin (1981*a*). The ratio $L_{\theta\theta,1}/L_{11,1}$ appears to approach an asymptotic value of 0.82 which is not very different from the values of 0.76 and 0.83 observed in the shear-flow measurements of Tavoularis & Corrsin (1981*a*) and the heated-grid experiments reported by Sreenivasan *et al.* (1980) respectively.

The Taylor microscales and the Corrsin microscale were evaluated according to the definitions

$$\lambda_{11} = \overline{U_1}\left[\frac{\overline{u_1^2}}{\overline{(\partial u_1/\partial t)^2}}\right]^{0.5}, \tag{5}$$

$$\lambda_{21} = \overline{U_1}\left[\frac{2\overline{u_2^2}}{\overline{(\partial u_2/\partial t)^2}}\right]^{0.5}, \tag{6}$$

$$\lambda_{\theta 1} = \overline{U_1}\left[\frac{2\overline{\theta^2}}{\overline{(\partial\theta/\partial t)^2}}\right]^{0.5}. \tag{7}$$

Figure 13(*a*) shows that the transverse distributions of the microscales λ_{11}, λ_{21} and $\lambda_{\theta 1}$ are fairly uniform although some values appear to increase slightly in the direction of the shear, as also observed by Tavoularis (1985). The downstream development of λ_{11}, λ_{21} and $\lambda_{\theta 1}$ (figure 13*b*) indicates the attainment of nearly constant asymptotic values, as observed in previous experiments (Tavoularis & Corrsin 1981*a*). The asymptotic values of the ratios $\lambda_{21}/\lambda_{11}$ and $\lambda_{\theta 1}/\lambda_{11}$ are 0.85 and 1.23, somewhat larger than the values 0.68 and 0.87 measured by Tavoularis & Corrsin (1981*a*).

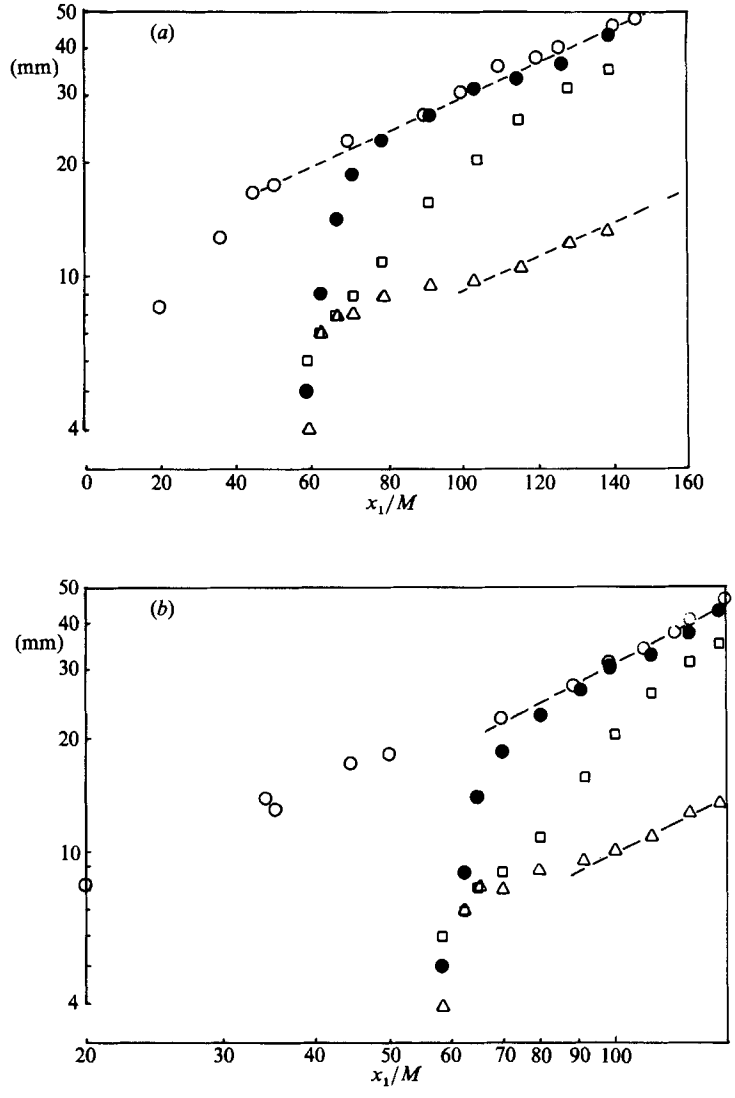

FIGURE 12. Downstream development of integral lengthscales along the centreline (*a*) in semilogarithmic coordinates, and (*b*) in logarithmic coordinates: ●, $L_{11,1}$; △, $L_{22,1}$; □, $L_{\theta\theta,1}$ (present measurements); ○, $L_{11,1}$ (from Tavoularis & Karnik 1988; no heating source).

3.5. *Skewness factors and temperature–velocity correlations*

The skewness factors for the two components of velocity were found to be less than 0.1 in magnitude sufficiently downstream from the source. Transverse profiles of the skewness factor of the temperature fluctuations, $S_\theta = \overline{\theta^3}/\theta'^3$, shown in figure 14, indicate that S_θ was positive, with a minimum value near the axis of the plume and decreasing in magnitude with distance from the source. A possible explanation will be given in the discussion.

Transverse profiles of the correlation coefficients $\rho_{u_1\theta} = \overline{u_1\theta}/u_1'\theta'$ and $\rho_{u_2\theta} = \overline{u_2\theta}/u_2'\theta'$ are presented in figure 15. These coefficients have opposite signs and they reverse signs near the location of the peak mean temperature. $\rho_{u_2\theta}$ is approximately -0.37 on the side of the lower velocity and 0.34 on the side of the higher velocity.

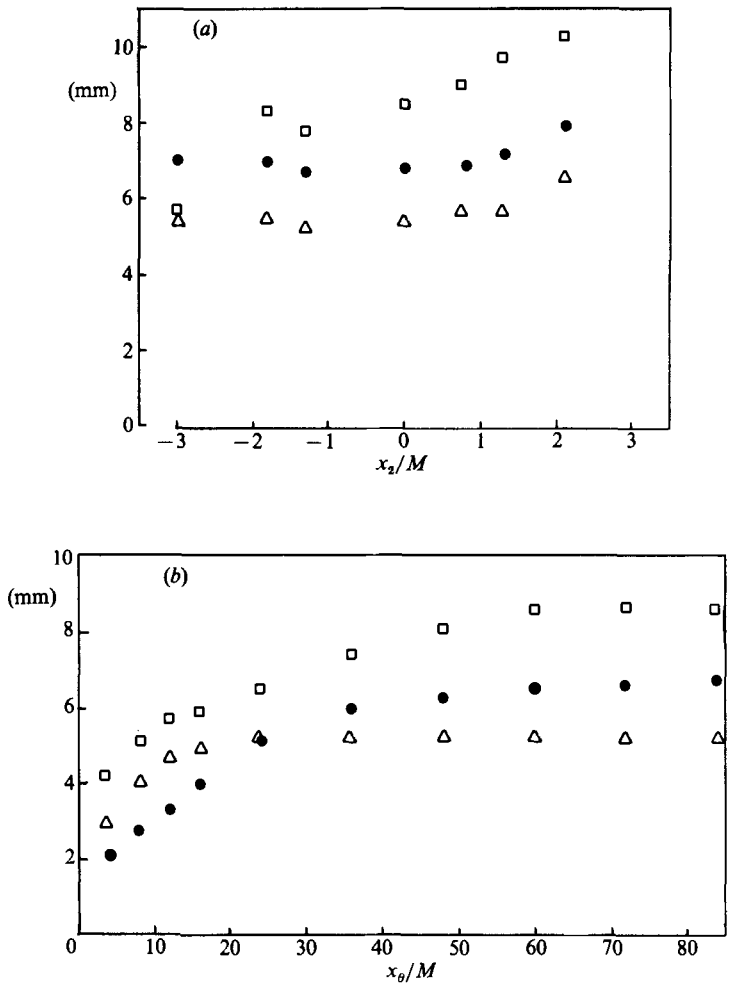

FIGURE 13. Measurements of the Taylor and Corrsin microscales. (*a*) Transverse distributions at $x_\theta/M = 84.0$, (*b*) downstream (centreline) development: ●, λ_{11}; △, λ_{21}; □, $\lambda_{\theta 1}$.

A similar behaviour has been observed in a related experiment performed by Sreenivasan *et al.* (1981) where the values changed from -0.5 to 0.35. Complementing this behaviour, $\rho_{u_1\theta}$ changes from about 0.44 on the side of lower velocity to -0.46 on the side of higher velocity.

Figure 16 presents transverse distributions of the triple correlation coefficients $\overline{\theta^2 u_1}/\overline{\theta^2}u_1'$ and $\overline{\theta^2 u_2}/\overline{\theta^2}u_2'$. As in the case of $\rho_{u_1\theta}$, the correlation coefficient $\overline{\theta^2 u_1}/\overline{\theta^2}u_1'$ (figure 16*a*) changes sign from positive values in the region of lower velocity to negative values in the region of higher velocity. However, the values in each region grow in magnitude away from the centreline and there appears to be a region of near constancy in the vicinity of the position of the mean temperature peak, before the change in sign occurs. Qualitatively, the transverse profile for $\overline{\theta^2 u_2}/\overline{\theta^2}u_2'$ (figure 16*b*) shows similar trends but is of opposite sign to the $\theta^2 u_1/\theta u_1'$ profile.

Transverse profiles for $\overline{u_1^2\theta}/\overline{u_1^2}\theta'$ and $\overline{u_2^2\theta}/\overline{u_2^2}\theta'$ are presented in figure 17. These profiles are very similar to each other and indicate a change in sign thrice; in the region of lower velocity, near the centreline and again in the region of higher velocity.

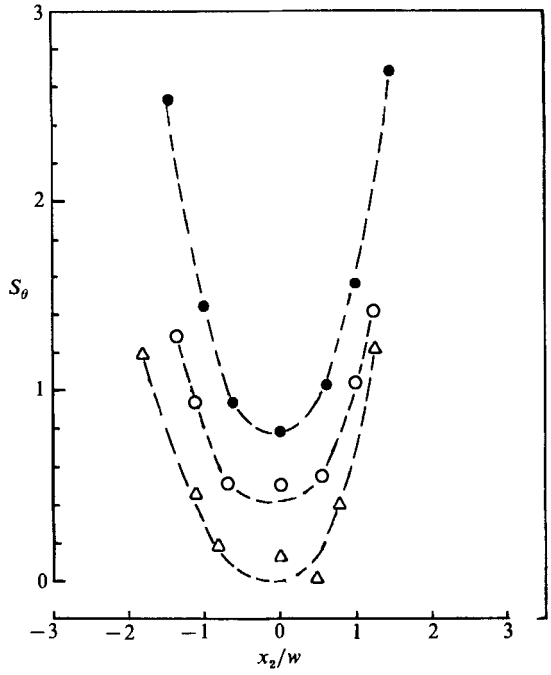

FIGURE 14. Transverse distribution of the skewness factor, S_θ, at $x_0/M = 24.0$ (●), 48.0 (○), 84.0(△).

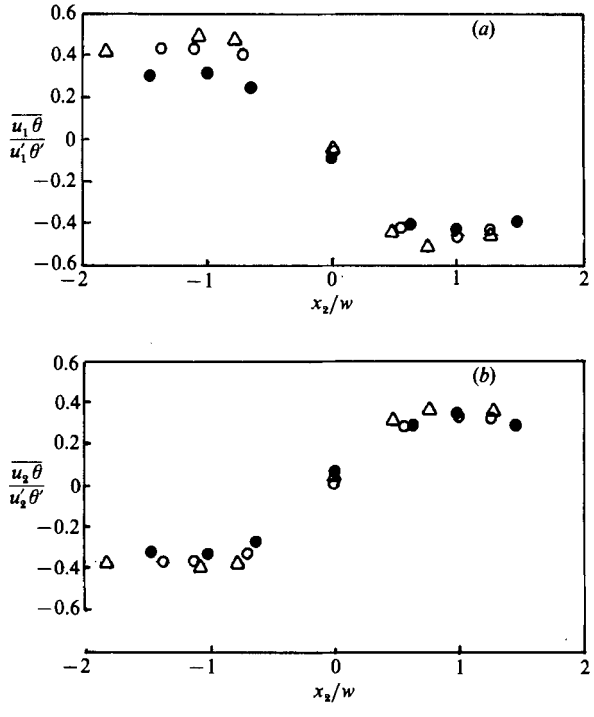

FIGURE 15. Transverse distribution of (*a*) $\overline{u_1\theta}/u_1'\theta'$, (*b*) $\overline{u_2\theta}/u_2'\theta'$; profiles at $x_0/M = 24.0$ (●), 48.0 (○), 84.0 (△).

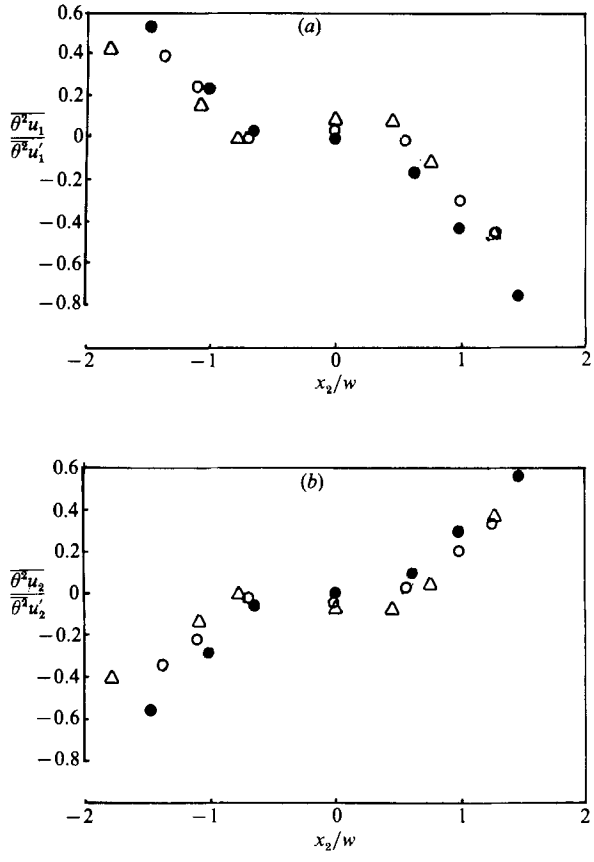

FIGURE 16. Transverse distribution of (*a*) $\overline{\theta^2 u_1}/\overline{\theta^2 u_1'}$, (*b*) $\overline{\theta^2 u_2}/\overline{\theta^2 u_2'}$. Symbols as in figure 15.

Finally, the profiles of $\overline{u_1 u_2 \theta}/u_1' u_2' \theta'$, shown in figure 18, appear to be a mirror image of the profiles in figure 17.

It is interesting to note that the transverse profiles of all the above correlations, measured at three downstream stations, nearly collapse when plotted versus the normalized distance x_2/w, implying a self-similar structure of the temperature field. Exact self-similarity is, of course, not attained, as evidenced, for example, by the developing skewness in the mean temperature profile and the growth of double peaks in the θ' profiles.

3.6. *Probability density functions*

The probability density functions (p.d.f.) of the two velocity components u_1 and u_2, shown in figure 19, closely match the standard normal density function also represented in the figure. Such a behaviour has also been observed by Tavoularis & Corrsin (1981*a*). On the other hand, the p.d.f. of the temperature fluctuation on the centreline shows a measurable deviation from the Gaussian p.d.f. and a skewness that increases with distance from the centreline (figure 20). The p.d.f. of θ at two positions with the same value of $\Delta\overline{T}/\Delta\overline{T}_p$ appear to be very close to each other.

The joint p.d.f. of the two velocity components, shown in figure 21, corroborates the observation of Tavoularis & Corrsin (1981*a*) that this quantity is not very different from a jointly normal p.d.f. with the same correlation coefficient. The joint

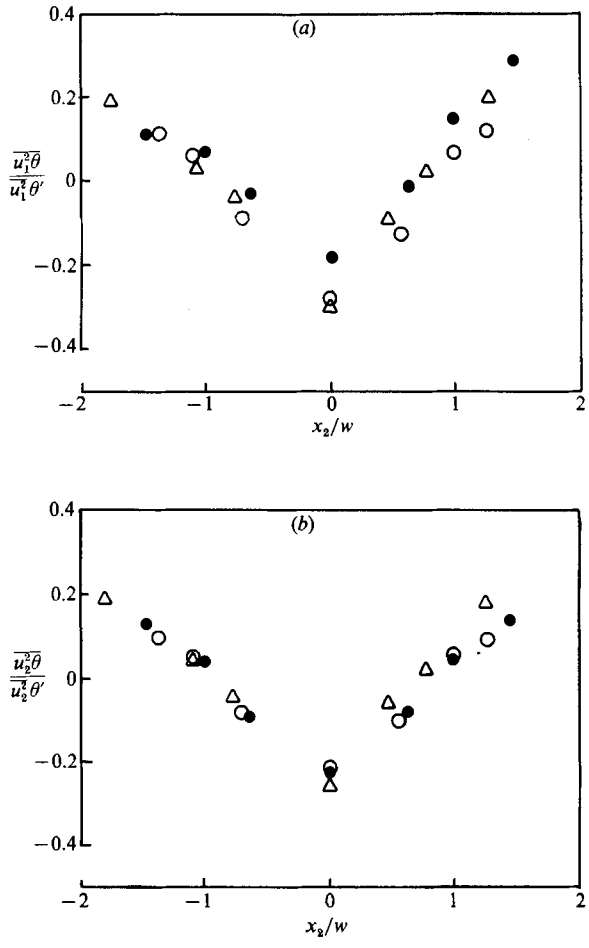

FIGURE 17. Transverse distribution of (*a*) $\overline{u_1^2\theta}/\overline{u_1^2}\theta'$, (*b*) $\overline{u_2^2\theta}/\overline{u_2^2}\theta'$. Symbols as in figure 15.

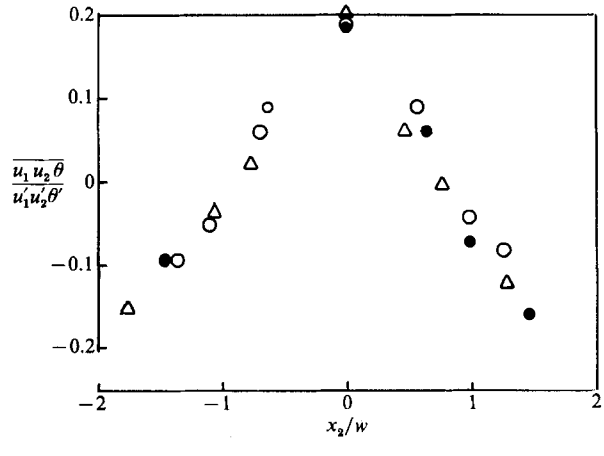

FIGURE 18. Transverse distribution of $\overline{u_1 u_2 \theta}/u_1' u_2' \theta'$. Symbols as in figure 15.

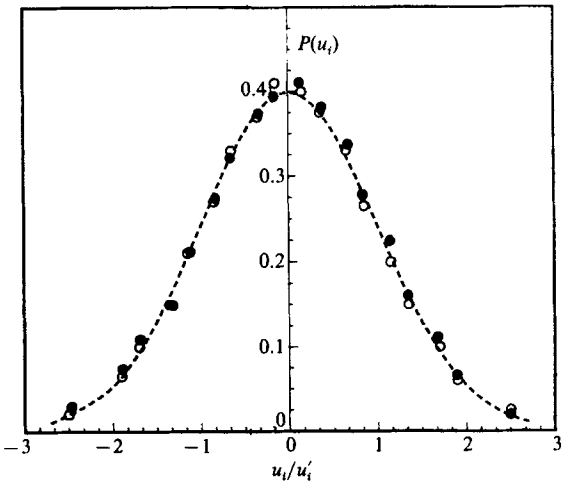

FIGURE 19. Probability density functions at $x_0/M = 84.0$, $x_2/M = 0$: $P(u_1)$ (○), $P(u_2)$ (●).

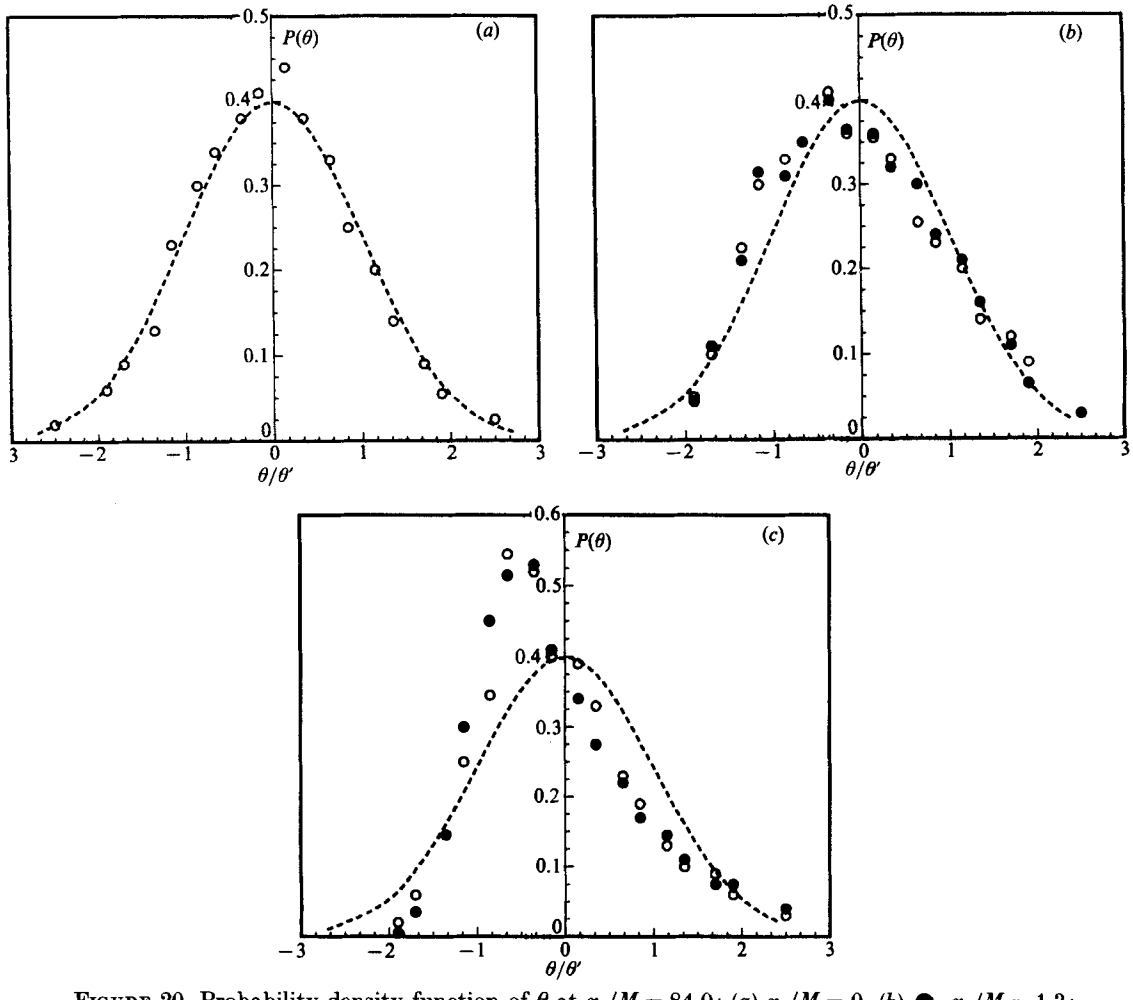

FIGURE 20. Probability density function of θ at $x_0/M = 84.0$: (*a*) $x_2/M = 0$, (*b*) ●, $x_2/M = 1.3$; ○, $x_2/M = -1.8$; (*c*) ●, $x_2/M = 2.1$; ○, $x_2/M = -3.0$.

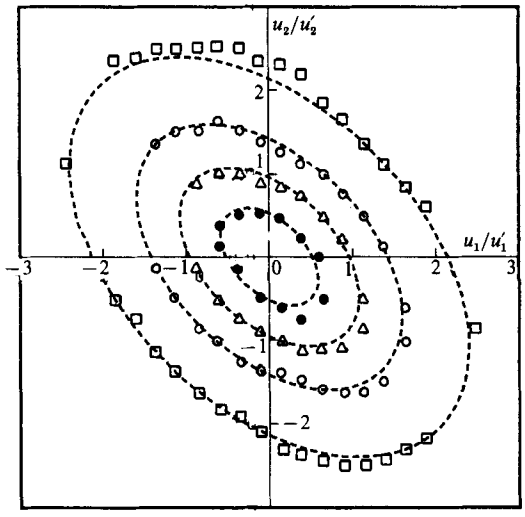

FIGURE 21. Joint probability contours of u_1 and u_2 at $x_\theta/M = 84.0$; $x_2/M = 0$: $P(u_1, u_2) = 0.15$ (●); 0.1 (△); 0.05 (○); 0.01 (□).

p.d.f. of each of the velocity components and the temperature fluctuations, shown in figure 22, indicate increasing deviation from a Gaussian behaviour with increasing distance from the centreline.

4. Discussion

4.1. *Test of passivity of heat input*

The electric power input to the line source was kept small in order to reduce the effect of heat injection upon the dynamics of the flow. Measurements of the velocity field behind the source, with and without heat, have not shown any appreciable differences. Nevertheless, the slight upward shift of the mean temperature peak near the heated wire could be attributed to buoyancy.

The magnitude of buoyancy effects was also examined by estimating the 'flux' and 'gradient' Richardson numbers. The flux Richardson number,

$$R_f = \frac{g}{\bar{T}} \frac{\overline{\theta u_2}}{\overline{u_1 u_2}\,(\mathrm{d}\bar{U}_1/\mathrm{d}x_2)}, \tag{8}$$

at the position of the maximum positive mean temperature gradient, varied from 0.022 to 0.0014 in the range $4 < x_\theta/M < 84$. Such values are much smaller than the critical value of 0.2, indicating that buoyancy effects were negligible in that range of x_θ/M. The gradient Richardson number,

$$R_g = \frac{g}{\bar{T}} \frac{\partial \bar{T}/\partial x_2}{(\mathrm{d}\bar{U}_1/\mathrm{d}x_2)^2}, \tag{9}$$

near the source ($x_\theta/M = 4$) attained values as high as 0.23, indicating the possibility of some buoyancy effects in that region. However, R_g decreased monotonically with downstream distance, to a value of 0.002 at $x_\theta/M = 84$, supporting the claim that heating effects were negligible and that heat could be treated as a passive contaminant.

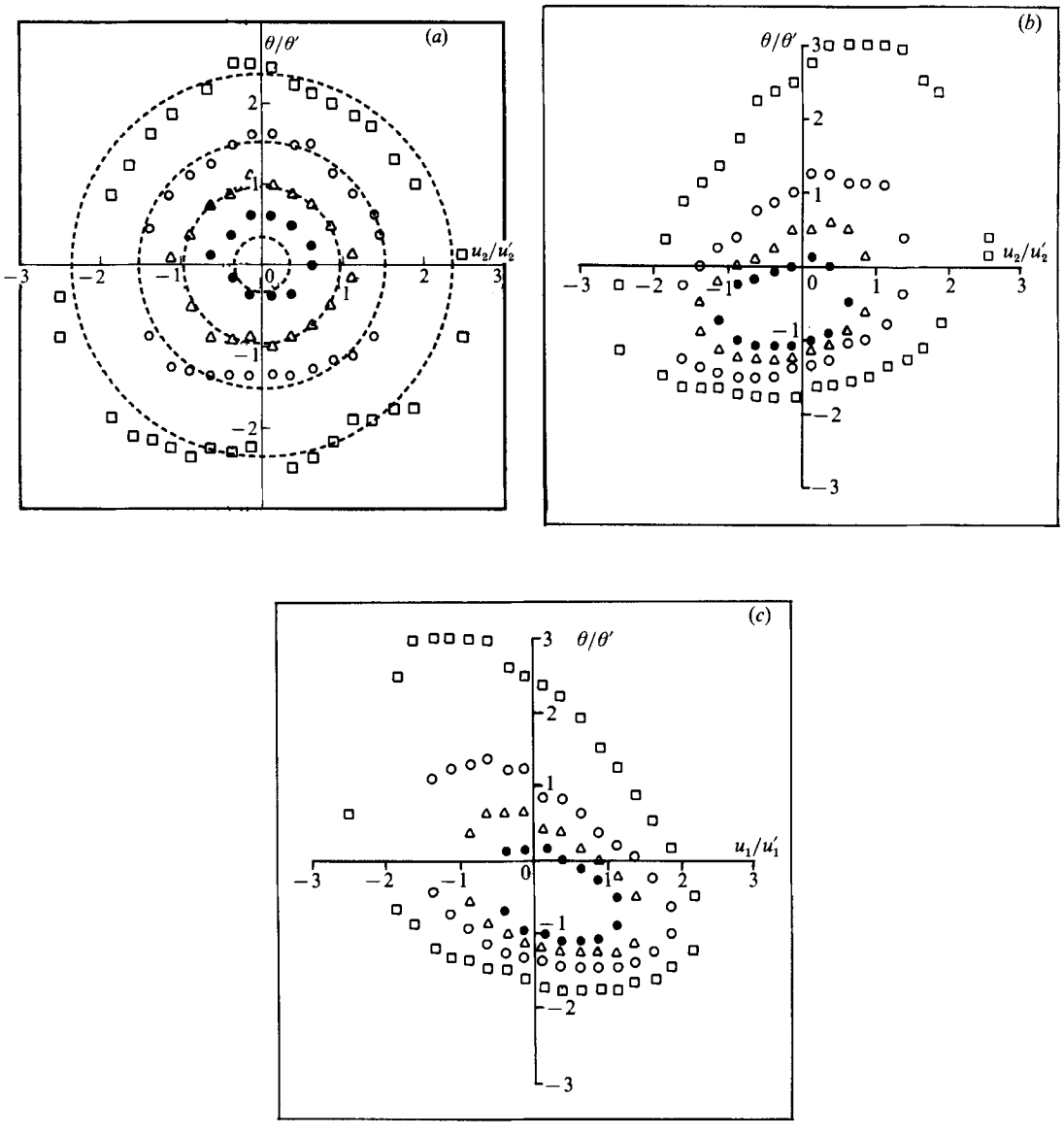

FIGURE 22. Joint probability contours of velocity components and temperature at $x_0/M = 84.0$: (*a*) $P(u_2, \theta)$ at $x_2/M = 0$; (*b*) $P(u_2, \theta)$ at $x_2/M = 2.1$; (*c*) $P(u_1, \theta)$ at $x_2/M = 2.1$. Symbols as in figure 21.

4.2. *Mean temperature profiles*

The development of the mean temperature profile due to a concentrated heat source in turbulent shear flows has been an issue of considerable debate. Simple physical argument leads to the expectation that, at a given distance downstream from the source, turbulent diffusion in eddies convected at a high mean speed would have acted upon the temperature field for less time than that in eddies convected at a low mean speed. If one further assumes that the turbulent diffusivity is uniformly distributed, one would expect that the heat should spread further into the low-velocity region than into the high-velocity region and that the position of maximum

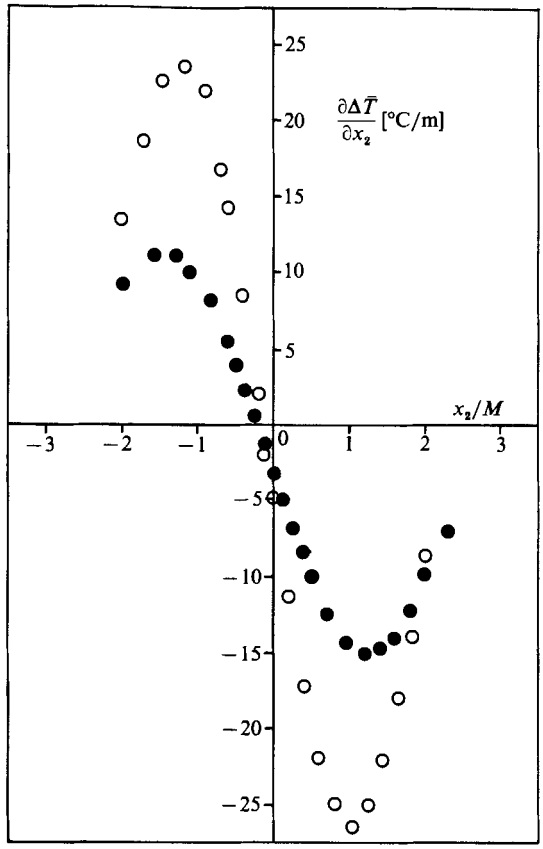

FIGURE 23. Transverse distribution of the mean temperature gradient computed by differentiating a fitted polynomial to the data of figure 6: ○, $x_\theta/M = 60.0$; ●, $x_\theta/M = 84.0$.

temperature should shift towards the high-velocity region. This argument has been supported by the computations of Okubo & Karweit (1969).

Consistent with the above argument, figures 6 and 7 reveal that, at a given x_θ, the spread of the isotherms with respect to the position of the peak mean temperature is greater in the region of low velocity than in the region of high velocity. The asymmetry of the mean temperature profile is illustrated more clearly in figure 23, showing the transverse mean temperature gradient distribution. Not only is the magnitude of this gradient generally higher on the high-speed side, but its asymmetry increases downstream, as evidenced, for example, by the increase of the ratio of maximum gradient magnitudes of the high-speed and low-speed sides from 1.13 at $x_\theta/M = 60$ to 1.33 at $x_\theta/M = 84$. A similar asymmetry in the mean temperature profiles has also been observed in the experiments of Tavoularis & Corrsin (1981*a*) and Nakamura *et al.* (1986).

On the other hand, measurements in a plane free jet and in a few other inhomogeneous shear flows, summarized by Hinze (1975), show a higher temperature spread towards the higher-speed side. This could be attributed to flow inhomogeneity and possibly to large-scale transport; the explanation provided by Hinze (1975) appears to be inconsistent with his mixing-length-type model. Finally, although the observation of Stapountzis & Britter (1987) of a symmetric profile, shifting towards

the high-speed side, seems contradictory at first glance, it is in fact compatible with the present measurements. This is because the only profile reported by Stapountzis & Britter (1987) was measured at a position corresponding to a total strain $\tau = (x_\theta/\bar{U}_{1c})(\mathrm{d}\bar{U}_1/\mathrm{d}x_2)$ of about 1.3. The present experiments also indicate that the mean temperature peak was on the high-speed side for $\tau < 2.5$, but it moved towards the low-speed side further downstream. Thus, the initial shift can be attributed to buoyancy, since the effects of shear on diffusion are expected to become measurable only after substantial straining of the flow. These effects are well documented by the present measurements, extending to regions with a total strain as large as 13.5.

Consideration of mean convection effects on diffusion would imply that the location of the peak mean temperature should move towards the high-velocity region. However, the present experiments, as well as those of Tavoularis & Corrsin (1981*a*), Nakamura *et al.* (1986) and Kyong & Chung (1987*a*) indicate that the locus of the peak mean temperature shifts monotonically towards the region of lower velocity. The possibility that the peak shift could be due to some spurious effect of the wind-tunnel air supply or the traversing system was further reduced by repeating some tests with the shear generator inverted so that the higher-velocity region was towards the lower half of the tunnel. These tests (not presented here) indicated once more that the mean temperature peak shifted towards the low-velocity region which was also the region of greater diffusion. This was also supported by the fact that the higher of the two peaks of the r.m.s. temperature profiles was in the higher-velocity side of the centreline. A clear explanation for this shift has not yet been found and it will be a topic of future investigations.

4.3. *Temperature fluctuations*

The phenomenon of the occurrence, suppression and subsequent reappearance of the double peaks in the r.m.s. temperature fluctuation profiles deserves further attention. Temperature fluctuations are produced 'locally' in regions of non-zero mean temperature gradient as well as transported from neighbouring regions by turbulent motions.

The ratio between the r.m.s. temperature fluctuations and the magnitude of the local mean temperature gradient, $|\partial\bar{T}/\partial x_2|$, shown in figure 24, is fairly constant away from the position of mean temperature peak (where it is by definition infinite), although θ' varies considerably across the flow. Constancy of this ratio is in perfect agreement with the concept of gradient transport in a transversely homogeneous turbulent field.

If local production were the only source of temperature fluctuations (and if one neglected production by the weak streamwise mean temperature gradient), then θ' should vanish at locations of peak mean temperature. This, however, does not happen because temperature fluctuations are also transported by turbulent eddies originating in regions with non-zero $\partial\bar{T}/\partial x_2$. Therefore, the size of these eddies relative to a scale characterizing the variation of $\partial\bar{T}/\partial x_2$ becomes an important parameter. If the size of transporting eddies is small compared with the distance over which $\partial\bar{T}/\partial x_2$ changes appreciably, local conditions prevail and θ' would be nearly proportional to the local value of $\partial\bar{T}/\partial x_2$. If, however, the size of these eddies is relatively large, the local value of θ' would also be affected by the mean temperature gradient at neighbouring locations and the θ' profile would tend to be smoother than that in the previous case. A possible measure of the relative eddy size is the ratio L_{11}/w, which has been plotted versus distance from the source in figure 25. The fact

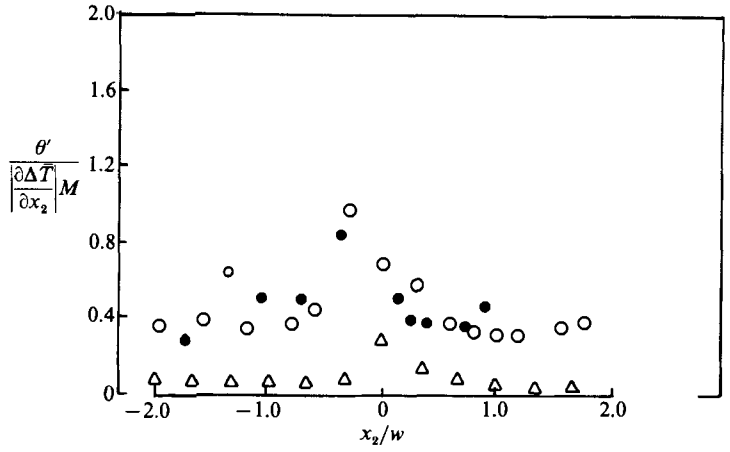

FIGURE 24. Transverse variation of the parameter $\theta'/(|\partial\Delta\bar{T}/\partial x_2|M)$; $x_0/M = 4.0$ (△), 48.0 (○), 84.0 (●).

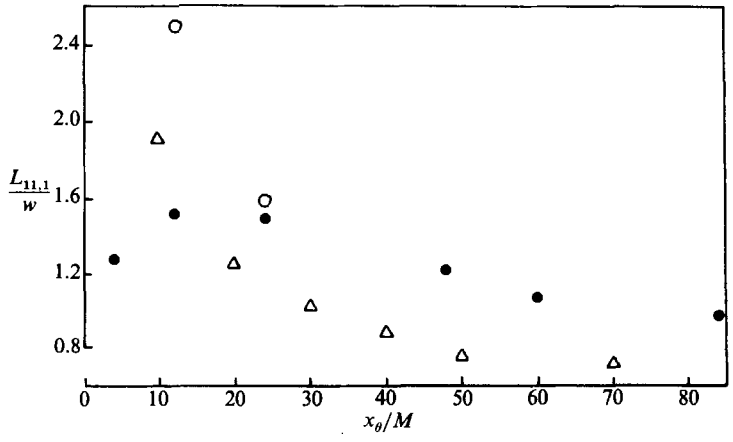

FIGURE 25. Downstream development of the ratio of the streamwise velocity lengthscale to the half-width of the mean temperature profile: ○, scale measured without ribbon; ●, scale measured with ribbon; △, Warhaft (1984).

that this ratio generally decreases away from the source is consistent with the increasing prominence of double peaks in the θ' profiles.

The above explanation can be further elucidated with the use of the following simplified model. Consider a Gaussian mean temperature profile, such that

$$\frac{\Delta\bar{T}}{\Delta\bar{T}_p} = e^{-z^2/2}, \tag{10}$$

where z is a dimensionless distance related to the location of the peak, x_{2p}, and the standard deviation of the profile, $\sigma = 0.85w$, by

$$z = \frac{x_2 - x_{2p}}{\sigma}. \tag{11}$$

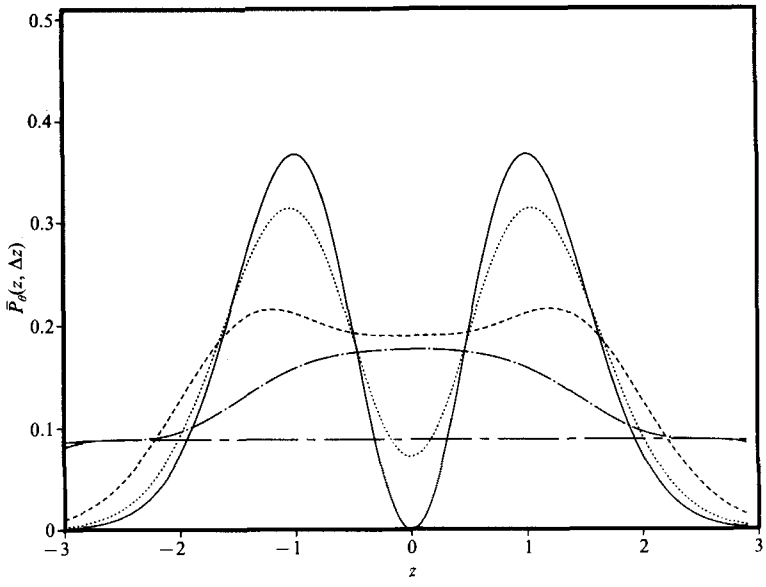

FIGURE 26. Spatially averaged production of temperature fluctuations for a Gaussian mean temperature profile: ——, $\Delta z = 0$; ....., $\Delta z = 1.0$; ----, $\Delta z = 2.0$; —·—, $\Delta z = 5.0$; —··—, $\Delta z = 10.0$.

Then, the local temperature fluctuation production, $P_\theta(z)$, can be expressed as

$$P_\theta(z) = -\overline{\theta u_2}\frac{\partial \bar{T}}{\partial x_2} \approx D_{22}\left(\frac{\partial \bar{T}}{\partial x_2}\right)^2 = \frac{D_{22}(\Delta \bar{T}_p)^2}{\sigma^2} z^2 \mathrm{e}^{-z^2}, \tag{12}$$

where D_{22} is the turbulent diffusivity that can be assumed to be a constant across the profile (see §4.5).

For a crude approximation one may assume that, at any given position, z, θ' is proportional to the production averaged over a span Δz, i.e.

$$\bar{P}_\theta(z, \Delta z) = \frac{1}{\Delta z}\int_{z-\frac{1}{2}\Delta z}^{z+\frac{1}{2}\Delta z} P_\theta(z)\,\mathrm{d}z \approx \frac{D_{22}(\Delta \bar{T}_p)^2}{\Delta z \sigma^2}\int_{z-\frac{1}{2}\Delta z}^{z+\frac{1}{2}\Delta z} z^2 \mathrm{e}^{-z^2}\,\mathrm{d}z, \tag{13}$$

where Δz could be considered to be analogous to the ratio $L_{11,1}/w$.

As seen in figure 26, for $\Delta z = 0$, $\bar{P}_\theta$ vanishes on the axis and has two prominent peaks. By analogy, one would expect that, when $L_{11,1}/w \approx 0, \theta' \approx 0$ where $\partial \bar{T}/\partial x_2 \approx 0$, i.e. at the peak of $\Delta \bar{T}$. As Δz increases, the value of $\bar{P}_\theta$ on the axis grows and its double peaks are suppressed. For sufficiently large Δz, a single peak occurs at the location $z = 0$, while, as $\Delta z \to \infty$, $\bar{P}_\theta$ becomes uniform. A similar behaviour would be expected for the θ' profile as a function of $L_{11,1}/w$.

The above model could be easily modified to incorporate the non-Gaussian features of the $\Delta \bar{T}$ profile or to introduce a weighted averaging of $\bar{P}_\theta$. This could lead to explanations of secondary observations, such as the fact that one peak in the θ' is higher than the other one.

4.4. *Temperature–velocity correlations*

Physical reasoning, based on the gradient transport concept, can be used to interpret, at least qualitatively, the variation of all measured temperature–velocity

correlations. It has already been demonstrated by several investigators that $\overline{u_2\theta}$ has a sign opposite to that of $\partial\overline{T}/\partial x_2$ in flows where this gradient dominates; in conformity with the negative correlation $\overline{u_1 u_2}$ in the present flow, $\overline{u_1\theta}$ is generally found to have the same sign as $\partial\overline{T}/\partial x_2$. A generalization of this concept to any transported quantity, a, leads to the general rule that the covariance $\overline{u_2 a}$ must have the opposite sign to and the covariance $\overline{u_1 a}$ the same sign as the mean gradient $\partial\overline{a}/\partial x_2$. This rule is adequate for explaining all present results. For example, the measured covariance $\overline{u_2^2\theta}$ is positive in regions with $\partial\overline{\theta u_2}/\partial x_2 < 0$, vanishes near the stationary points of $\overline{\theta u_2}$ (nearly coinciding with the inflection points of the mean temperature profile) and is negative in regions with $\partial\overline{\theta u_2}/\partial x_2 > 0$ (e.g. around the centreline). Similar explanations can be devised for the variations of $\overline{u_1\theta^2}$, $\overline{u_2\theta^2}$, $\overline{u_1^2\theta}$, and $\overline{u_1 u_2\theta}$.

On the other hand, the positive sign of the triple moment $\overline{\theta^3}$ (and, thus, of the temperature fluctuation skewness, S_θ) is due to an entirely different reason. At first, one may observe that positive skewness of a random variable corresponds to a non-Gaussian distribution in which negative peaks of the variable occur with smaller amplitude but longer total duration than the positive peaks. In the present situation, the fluctuating temperature is bounded between the unheated, ambient fluid temperature and the heating source temperature, although fluid with intermediate temperatures is produced at different positions in the thermal plume of the source as a result of molecular diffusion and mixing. The observed positive skewness of θ is attributed to the occurrence of low-amplitude negative peaks in the θ-signal, corresponding to the 'cold' fluid. This also explains why S_θ increases dramatically from the centreline towards the edges of the plume. The fact that S_θ decreases monotonically downstream is due to the smearing out of hot-fluid positive temperature peaks by molecular diffusion.

4.5. *Turbulent diffusivities*

The applicability of a turbulent diffusivity tensor, D_{ij}, defined as

$$\overline{\theta u_i} = -D_{ij}\frac{\partial\overline{T}}{\partial x_j}, \tag{14}$$

to nearly homogeneous shear flows has been established by the experiments of Sreenivasan *et al.* (1981) and Tavoularis & Corrsin (1981*a*, 1985). Estimates of the components of D_{ij} (Tavoularis & Corrsin 1985) indicate that the tensor is neither diagonal nor symmetric.

Although, in the present flow, both $\partial\overline{T}/\partial x_2$ and $\partial\overline{T}/\partial x_1$ are generally non-zero, the former gradient is much larger than the latter, except within a narrow region around the peak of the mean temperature profile. With this consideration and in view of the appreciable turbulent transport into regions with small $\partial\overline{T}/\partial x_2$, estimates of D_{11} and D_{21} are subject to large errors and will not be presented here.

The D_{12} and D_{22} components, evaluated in regions where $|\partial\overline{T}/\partial x_2| \gg |\partial\overline{T}/\partial x_1|$, showed relatively small transverse variation. Their ratio, D_{12}/D_{22}, throughout the heated region, was remarkably close to the value of 2.1 measured by Tavoularis & Corrsin (1985).

Turbulent diffusivities in homogeneous flows can be expressed as products of a Lagrangian characteristic velocity and a Lagrangian characteristic length (Corrsin 1957). In the absence of Lagrangian measurements one could estimate D_{22} from the producer of the Eulerian scales u_2' and L_{11}. The ratio $D_{22}/(u_2' L_{11})$ was about 0.1, in

	Estimates of D_{22} (m^2/s)				Estimates of D_{12}/D_{22}			
$\frac{X_2}{M}$	$\frac{\overline{u_2\theta^2}}{\partial\overline{T}/\partial x_2}$	$\frac{\overline{u_2\theta^2}}{\partial\overline{\theta^2}/\partial x_2}$	$\frac{\overline{u_1u_2\theta}}{\partial\overline{u_1\theta}/\partial x_2}$	$\frac{\overline{u_2^2\theta}}{\partial\overline{u_2\theta}/\partial x_2}$	$\frac{\overline{u_1\theta}}{\overline{u_2\theta}}$	$\frac{\overline{u_1\theta^2}}{\overline{u_2\theta^2}}$	$\frac{\overline{u_1^2\theta}}{\overline{u_1u_2\theta}}$	$\frac{\overline{u_1u_2\theta}}{\overline{u_2^2\theta}}$
0	—	—	0.0033	0.0035	—	—	−2.3	−1.3
2.1	0.0016	0.0024	—	—	−2.0	−1.9	—	—
−1.8	0.0025	0.0016	—	—	−2.0	−1.8	—	—

TABLE 1. Typical estimates of diffusivities at $x_0/M = 84.0$

close agreement with the measurements of Sreenivasan *et al.* (1981) and Tavoularis & Corrsin (1981*a*).

Following the successful qualitative explanation (§4.4) of the signs of the third-order temperature–velocity correlations, one could further explore the applicability of simple gradient transport models to the prediction of third moments. Since the transport mechanism is the same for all quantities, one is tempted to consider the use of identical diffusivities for the corresponding second and third-order covariances, as

$$\overline{u_i u_k \theta} = -D_{ij}\frac{\partial\overline{u_k\theta}}{\partial x_j}, \tag{15}$$

$$\overline{u_i \theta^2} = -D_{ij}\frac{\partial\overline{\theta^2}}{\partial x_j}. \tag{16}$$

As seen in table 1, the values of the central diffusivity, D_{22}, estimated from the three third-order covariances, are not very different from that estimated from the heat flux. Also, the ratios of the two measurable components of the turbulent diffusivity tensor, D_{12}/D_{22}, were comparable in both cases. Thus, it appears that a universal turbulent diffusivity tensor could be used for rough estimates of both second- and third-order temperature–velocity correlations.

5. Conclusions

The main conclusions of the present study can be summarized as follows.

(*a*) At sufficiently large diffusion times the mean shear causes the mean temperature profile to become asymmetric and its peak to shift towards the region of lower velocity.

(*b*) The occurrence, suppression and reappearance of the double peaks in the temperature fluctuation profiles can be explained by considering the relative size of energy-containing eddies with respect to the plume width.

(*c*) The variations of double and triple temperature–velocity correlations are consistent with the gradient transport concept. A universal turbulent diffusivity tensor can be used to model all these quantities.

(*d*) The positive temperature fluctuation skewness can be attributed to the effect of negative fluctuations in the signal due to 'cold' fluid.

(*e*) The collapse of the temperature–velocity correlations at various downstream stations indicates an approach to a self-similar temperature field, although exact self-similarity is precluded by the monotonic development of the mean and r.m.s. temperature profiles.

REFERENCES

ALEXOPOULOS, C. C. & KEFFER, J. F. 1971 Turbulent wake in a passively stratified field. *Phys. Fluids* **14**, 216.

ANAND, M. S. & POPE, S. B. 1983 Diffusion behind a line source in grid turbulence. In *Proc. Fourth Symp. Turb. Shear Flows, Karlsruhe* (ed. L. J. S. Bradbury *et al.*), p. 17.11. Springer.

BUDWIG, R., TAVOULARIS, S. & CORRSIN, S. 1985 Temperature fluctuations and heat flux in grid generated isotropic turbulence with streamwise and transverse mean temperature gradients. *J. Fluid Mech.* **153**, 441.

CHAMPAGNE, F. H., HARRIS, V. G. & CORRSIN, S. 1970 Experiments on nearly homogeneous turbulent shear flow. *J. Fluid Mech.* **41**, 81.

COLLIS, D. C. 1948 The diffusion process in turbulent flow. *Rep.* A55. Div. Aero. Australian Council Sci. and Indus. Res.

CORRSIN, S. 1952 Heat transfer in isotropic turbulence. *J. Appl. Phys.* **23**, 113.

CORRSIN, S. 1957 Some current problems in turbulent shear flow. In *Naval Hydrodynamics, Proc. 1st Symp. on Naval Hydrodynamics, Publication* 515, p. 373.

DEISSLER, R. G. 1962 Turbulent heat transfer and temperature fluctuations in a field with uniform velocity and temperature gradients. *Intl J. Heat Mass Transfer* **6**, 257.

ELRICK, D. E. 1962 Source functions for diffusion in uniform shear flow. *Austral. J. Phys.* **15**, 283.

FOX, J. 1964 Turbulent temperature fluctuations and two dimensional heat transfer in a uniform shear flow. *NASA Tech. Note* D2511.

FRENKIEL, F. N. 1950 On turbulent diffusion. *Symp. on Turbulence, Naval Ord. Lab., Rep.* 1136, p. 67.

HARRIS, V. G., GRAHAM, J. A. & CORRSIN, S. 1977 Further experiments in nearly homogeneous turbulent shear flow. *J. Fluid Mech.* **81**, 657.

HINZE, J. O. 1975 *Turbulence*, 2nd edn. McGraw-Hill.

HUANG, C. H. 1979 A theory of dispersion in turbulent shear flow. *Atmos. Environ.* **13**, 453.

JONES, W. P. & MUSONGE, M. 1983 Modelling of scalar transport in homogeneous turbulent flows. In *Proc. Fourth Symp. on Turbulent Shear Flows, Karlsruhe* (ed. L. J. S. Bradbury, *et al.*), p. 17.18. Springer.

KARNIK, U. & TAVOULARIS, S. 1987 Generation and manipulation of uniform mean shear with the use of screens. *Exp. Fluids* **5**, 247.

KISTLER, A. L. 1956 Measurement of joint probability in turbulent dispersion of heat from two line sources. PhD dissertation, part II, The Johns Hopkins University, Baltimore, USA.

KISTLER, A. L., O'BRIEN, V. & CORRSIN, S. 1956 Double and triple correlations behind a heated grid. *J. Aero Sci.* **23**, 96.

KYONG, H. N. & CHUNG, K. M. 1987*a* Measurements of turbulent diffusion field behind a line heat source in a homogeneous shear flow. *Korean Soc. Mech. Engrs J.* **1**, 24.

KYONG, H. N. & CHUNG, K. M. 1987*b* Turbulent scalar transport correlation behind a line heat source in a uniform shear flow. *Korean Soc. Mech. Engrs J.* **1**, 95.

LIBBY, P. & SCRAGG, C. 1972 Diffusion of heat from a line source downstream of a turbulence grid. *Amer. Inst. Aeron. Astron. J.* 562.

LIN, S. C. & LIN, S. C. 1973 Study of strong temperature mixing in subsonic grid turbulence. *Phys. Fluids* **16**, 1587.

LUMLEY, J. L. 1978 Computational modelling of turbulent flows. *Adv. Appl. Mech.* **18**, 123.

LUMLEY, J. L. 1983 Turbulence modelling. *Trans. ASME* E: *J. Appl. Mech.* **105**, 1097.

LUMLEY, J. L. & VAN CRUYNINGEN, I. 1985 Limitations of second order modelling of passive scalar diffusion. In *Frontiers in Fluid Mechanics* (ed. S. H. Davis & J. L. Lumley), p. 199. Springer.

MILLS, R., KISTLER, A. L., O'BRIEN, V. & CORRSIN, S. 1958 Turbulence and temperature fluctuations behind a heated grid. *NACA Tech. Note* 4288.

MILLS, R. R. & CORRSIN, S. 1959 Effect of contraction on turbulence and temperature fluctuations generated by a warm grid. *NASA Memo.* 5-5-59W.

MONIN, A. S. & YAGLOM, A. M. 1973 *Statistical Fluid Mechanics*. MIT Press.

NAKAMURA, I., SAKAI, Y., MIYATA, M. & TSUNODA, H. 1986 Diffusion of matter from a continuous point source in uniform mean shear flows. *Bull. JSME* **29**, 1141.

NEWMAN, G. R., WARHAFT, Z. & LUMLEY, J. L. 1977 The decay of temperature fluctuations in isotropic turbulence. *Proc. 6th Australasian Hydraulics and Fluid Mech. Conf., Adelaide.*

NOVIKOV, E. A. 1958 Turbulent diffusion in a shear flow. *Prikl. Mat. Mekh.* **22**, 412.

OKUBO, A. & KARWEIT, M. J. 1969 Diffusion from a continuous source in a uniform shear flow. *Limnol. Oceanogr.* **14**, 514.

POPE, S. B. 1981 Transport equation for the joint probability density function of velocity and scalars in turbulent flow. *Phys. Fluids* **24**, 588.

POPE, S. B. 1983 Consistent modelling of scalars in turbulent flows. *Phys. Fluids* **26**, 404.

RILEY, J. & CORRSIN, S. 1971 Simulation and computation of dispersion in turbulent shear flow. *Proc. Conf. on Air Pollut. Met., Amer. Met. Soc.*, p. 16.

RILEY, J. & CORRSIN, S. 1974 The relation of turbulent diffusivities to Lagrangian statistics for the simplest shear flow. *J. Geophys. Res.* **79**, 1768.

ROGERS, M. M., MOIN, P. & REYNOLDS, W. C. 1986 The structure and modeling of hydrodynamic and scalar fields in homogeneous turbulent shear flow. *Dept. of Mech. Engng Rep.* TF-25. Stanford University, Stanford, California.

SAKAI, Y., NAKAMURA, I., MIYATA, M. & TSUNODA, H. 1986 Diffusion of matter from a continuous point source in uniform mean shear flows (2nd report). *Bull. JSME* **29**, 1149.

SCHUBAUER, G. B. 1935 A turbulence indicator utilizing the diffusion of heat. *NACA Rep.* 524.

SEPRI, P. 1976 Two-point turbulence measurements downstream of a heated grid. *Phys. Fluids* **19**, 1876.

SHIH, T. H. & LUMLEY, J. L. 1986 Influence of timescale ratio on scalar flux relaxation: modelling Sirivat and Warhaft's homogeneous passive scalar fluctuations. *J. Fluid Mech.* **162**, 211.

SHIRANI, E., FERZIGER, J. H. & REYNOLDS, W. C. 1981 Mixing of a passive scalar in isotropic and sheared homogeneous turbulence. *Dept. Mech. Engng Rep.* TF-15, Stanford University, Stanford, California.

SHLIEN, D. J. & CORRSIN, S. 1974 A measurement of Lagrangian velocity autocorrelation in approximately isotropic turbulence. *J. Fluid Mech.* **62**, 255.

SIRIVAT, A. & WARHAFT, Z. 1983 The effect of a passive cross-stream temperature gradient on the evolution of temperature variance and heat flux in grid turbulence. *J. Fluid Mech.* **128**, 323.

SREENIVASAN, K. R., TAVOULARIS, S. & CORRSIN, S. 1981 A test of gradient transport and its generalizations. In *Turbulent Shear Flows*, vol. 3 (ed. L. J. S. Bradbury *et al.*), p. 96. Springer.

SREENIVASAN, K. R., TAVOULARIS, S., HENRY, R. & CORRSIN, S. 1980 Temperature fluctuations and scales in grid turbulence. *J. Fluid Mech.* **100**, 597.

STAPOUNTZIS, H. & BRITTER, R. E. 1987 Turbulent diffusion behind a heated line source in a nearly homogeneous turbulent shear flow. *Proc. Sixth Symp. on Turbulent Shear Flows, Toulouse*, p. 9.2.1. Springer.

STAPOUNTZIS, H., SAWFORD, B. L., HUNT, J. C. R. & BRITTER, R. E. 1986 Structure of the temperature field downwind of a line source in grid turbulence. *J. Fluid Mech.* **165**, 401.

SULLIVAN, P. 1976 Dispersion of a line source in grid turbulence. *Phys. Fluids* **19**, 159.

TAVOULARIS, S. 1978 A circuit for the measurement of instantaneous temperature in heated turbulent flows. *J. Sci. Instrum.* **11**, 21.

TAVOULARIS, S. 1985 Asymptotic laws for transversely homogeneous turbulent shear flows. *Phys. Fluids* **28**, 999.

TAVOULARIS, S. & CORRSIN, S. 1981*a* Experiments in a nearly homogeneous shear flow with a uniform mean temperature gradient. Part 1. *J. Fluid Mech.* **104**, 311.

TAVOULARIS, S. & CORRSIN, S. 1981*b* Experiments in nearly homogeneous turbulent shear flow with a uniform mean temperature gradient. Part 2. The fine structure. *J. Fluid Mech.* **104**, 349.

TAVOULARIS, S. & CORRSIN, S. 1985 Effects of shear on the turbulent diffusivity tensor. *Intl J. Heat Mass Transfer* **28**, 265.

TAVOULARIS, S. & KARNIK, U. 1989 Further experiments on the evolution of turbulent stresses and scales in uniformity sheared turbulence. *J. Fluid Mech.* (submitted).

TAYLOR, G. I. 1921 Diffusion by continuous movements. *Proc. Lond. Math. Soc.* A **20**, 196.

TOWNSEND, A. A. 1951 The diffusion of heat spots in isotropic turbulence. *Proc. R. Soc. Lond.* A **209**, 418.

TOWNSEND, A. A. 1954 The diffusion behind a line source in homogeneous turbulence. *Proc. R. Soc. Lond.* A **224**, 487.

UBEROI, M. S. & CORRSIN, S. 1952 Diffusion from a line source in isotropic turbulence. *NACA Tech. Note* 2710 (also *NACA Rep.* 1142).

VENKATARAMANI, K. S. & CHERVAY, R. 1978 Statistical features of heat transfer in grid generated turbulence: constant gradient case. *J. Fluid Mech.* **86**, 513.

WARHAFT, Z. 1981 The use of dual injection to infer scalar covariance decay in grid turbulence. *J. Fluid Mech.* **104**, 93.

WARHAFT, Z. 1984 The interference of thermal fields from line sources in grid turbulence. *J. Fluid Mech.* **144**, 363.

WARHAFT, Z. & LUMLEY, J. L. 1978 An experimental study of the decay of temperature fluctuations in grid generated turbulence. *J. Fluid Mech.* **88**, 659.

WISKIND, H. K. 1962 A uniform gradient turbulent transport experiment. *J. Geophys. Res.* **67**, 3033.

YEH, T. T. & VAN ATTA, C. W. 1973 Spectral transfer of scalar and velocity fields in heated grid turbulence. *J. Fluid Mech.* **58**, 233.